arXiv:1512.04146v1 [cond-mat.mes-hall] 14 Dec 2015

Nonlocal Anomalous Hall Effect

Steven S.-L. Zhang and Giovanni Vignale
Department of Physics and Astronomy, University of Missouri, Columbia, MO 65211
(Dated: December 15, 2015)

The anomalous Hall effect is deemed to be a unique transport property of ferromagnetic metals, caused by the concerted action of spin polarization and spin-orbit coupling. Nevertheless, recent experiments have shown that the effect also occurs in a nonmagnetic metal (Pt) in contact with a magnetic insulator (yttrium iron garnet (YIG)), even when precautions are taken to ensure there is no induced magnetization in the metal. We propose a theory of this effect based on the combined action of spin-dependent scattering from the magnetic interface and the spin Hall effect in the bulk of the metal. At variance with previous theories, we predict the effect to be of first order in the spin-orbit coupling, just as the conventional anomalous Hall effect – the only difference being the spatial separation of the spin orbit interaction and the magnetization. For this reason we name this effect *nonlocal anomalous Hall effect* and predict that its sign will be determined by the sign of the spin Hall angle in the metal. The AH conductivity that we calculate from our theory is in good agreement with the measured values in Pt/YIG structures.

Introduction.– The anomalous Hall (AH) effect is the generation of an electric current perpendicular to the electric field in a ferromagnetic metal [1]. At variance with the ordinary Hall effect, which arises from the action of a magnetic field on the orbital

motion of the electrons, the AH effect is ascribed to strong spin-orbit coupling in concert with spin-polarized itinerant electrons. The spin orbit coupling plays a central role in inducing a left-right asymmetry (with respect to the direction of the electric field) in the scattering of electrons of opposite spins. It is this asymmetry that generates a transverse charge current from a longitudinal spin current. The same scattering process generates a pure transverse spin current for systems with spin unpolarized electrons, which is known as spin Hall effect [2–5]. Based on this picture, the conventional AH effect appears at *first order* in spin orbit coupling, no matter which kind of microscopic mechanisms predominates.

Recently, an AH signal has also been detected in a Platinum (Pt) layer in direct contact with a YIG layer [6–8]. The former is a non-magnetic heavy metal with strong spin orbit coupling and the latter is a well-known ferromagnetic insulator. In view of the two aforementioned ingredients for the AH effect in ferromagnets, it is puzzling that an AH current would arise in Pt in the absence of spin polarized conduction electrons. In a first attempt to solve the puzzle, Huang et. al. [6] showed that the Pt layer in close proximity with YIG acquires ferromagnetic characteristics, which essentially subsumes the novel AH effect under the conventional AH effect for ferromagnetic metals. This explanation ran into difficulties when it was found that the AH effect persists in Pt/Cu/YIG trilayers [9] where the Cu layer is deliberately inserted to eliminate the magnetic proximity effect.

An alternative explanation was then proposed [9, 10], based on the physical mechanism depicted in panel (a) of Fig. 1. In this mechanism the applied charge current j_x generates, via the spin Hall effect, a spin current Q^y_z propagating in the $z-$direction with spin along the $y-$ direction. When those electrons carrying Q^y_z are reflected back from the magnetic interface, spin rotation occurs and gives rise to a spin current of Q^x_z, which in turn induces a transverse charge current j_y via the inverse spin Hall effect [11, 12]. Based on this picture, the transverse electric current is of *second order* in the spin orbit coupling or spin Hall angle, which is qualitatively different from a conventional AH current. It is worth mentioning that a fit to the experimental data based on this model [7, 10], requires a spin diffusion length on the order of 1 nm. Such a short spin diffusion length, an order of magnitude smaller than the room-temperature electron mean path of Pt [13], casts doubt on the internal consistency of the spin diffusion model.

In this paper, we propose a different mechanism for the AH current observed in hybrid heavy-metal/ferromagnetic-insulator structures. The essential new ingredient is the scattering of electrons from the (rough) metal-insulator interface. Because the insulator is magnetic, the scattering rate is spin-dependent (see Appendix B for a proof). This means that a charge current flowing parallel to the interface is partially converted to a spin current, while a spin current flowing parallel to the interface is partially converted to a charge current. The surface-induced conversion of charge to spin current and viceversa conspires with the spin Hall effect in the bulk of the metal to produce the observed AH current. This may happen in two ways: in the first process, (b1), the charge current j_x generates, via spin-dependent interfacial scattering a spin current Q^z_x, which subsequently gives rise to the transverse spin polarized current j_y via the inverse spin Hall effect; in the second process, (b2),

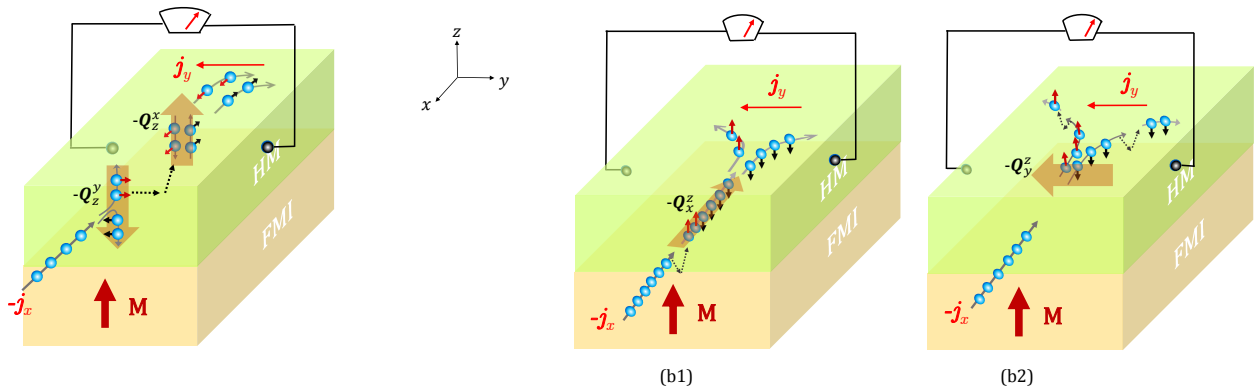

(a) Spin Hall AH effect ($\propto \theta_{sh}^2$)

(b1) (b2)

(b) Nonlocal AH effect ($\propto \theta_{sh}$)

FIG. 1: Schematics of two different mechanisms of the AH effect in heavy-metal (HM)/ferromagnetic-insulator (FMI) bilayers: (a) the spin Hall AH mechanism and (b) nonlocal AH mechanism with two coexisting physical processes depicted separately in panels b1 and b2. The curved arrows represent the trajectories of electrons upon spin orbital scattering and the dotted arrows stand for spin dependent scattering at the magnetic interface.

the applied charge current j_x first generates, via spin Hall effect, a transverse spin current Q_y^z, which is then turned into a spin polarized current j_y due to spin dependent interfacial scattering. Both physical processes involve spin orbit scattering only once (through the spin Hall effect) and hence the resulting AH current is of *first order* in the spin orbit coupling or spin Hall angle. As a matter of fact, this AH effect has the same physical nature as its conventional counterpart in bulk ferromagnets, and differs from the latter only in the spatial separation of the spin orbit interaction and the magnetization: it is for this reason that we name it *nonlocal AH effect*.

Compared to the double spin Hall effect mechanism proposed in Refs. [9, 10], our proposal replaces one of the spin Hall steps, the first or the second, by a spin-dependent interfacial scattering. This leads to a good quantitative description of the transverse current without the need of introducing an exceedingly small spin diffusion length, as we will show in details in the remainder of the paper. In fact, our mechanism survives in the limit of infinite spin diffusion length, while the double spin Hall effect mechanism vanishes in that limit [10]. In addition, the new mechanism has distinctive features that can be tested experimentally, the most striking one being the sign of the effect, which we predict to track the sign of the bulk spin Hall angle.

Linear response theory—Let us consider a metal/insulator bilayer as shown in Fig. 1 with an external electric field applied in the $x-$direction (i.e., $\mathbf{E}_{ext} = E_{ext}\hat{\mathbf{x}}$) and with the magnetization of the insulator layer pointing in the z direction, i.e., $\mathbf{m} = \hat{\mathbf{z}}$. We also assume that both surfaces of the metal are rough, but on the average translational invariance is recovered so that the transport properties are independent of x and y coordinates. The linear response of current densities to spin dependent electric fields can be written as follows

$$\begin{aligned} \mathbf{j}(z) &= C_0\mathbf{E}(z) + C_s\boldsymbol{\mathcal{E}}_{\parallel}(z) \\ \mathbf{Q}_{\parallel}(z) &= C_0\boldsymbol{\mathcal{E}}_{\parallel}(z) + C_s\mathbf{E}(z) \\ \mathbf{Q}_{\perp}(z) &= C_r'\boldsymbol{\mathcal{E}}_{\perp}(z) + C_r''\hat{\mathbf{z}}\times\boldsymbol{\mathcal{E}}_{\perp}(z) \end{aligned} \tag{1}$$

where $\mathbf{j}(z) = (j_x, j_y)$ is the in-plane current density (note that $j_z = 0$ everywhere in the metal layer due to the open boundary conditions), $\mathbf{Q}_{\parallel} = (Q_x^z, Q_y^z)$ is the in-plane spin-current density (with spin in the z direction), and $\mathbf{Q}_{\perp} = (Q_z^x, Q_z^y)$ is the perpendicular-to-plane spin current density with Q_z^x and Q_z^y carrying the x and y components of the spin. The corresponding fields are $\mathbf{E} = (E_x, E_y)$, $\boldsymbol{\mathcal{E}}_{\parallel} = (\mathcal{E}_x^z, \mathcal{E}_y^z)$ and $\boldsymbol{\mathcal{E}}_{\perp} = (\mathcal{E}_z^x, \mathcal{E}_z^y)$. Notice that C_k is defined as the integral operator with kernel $c_k(z, z')$, i.e., $C_k f(z) \equiv \int \mathrm{d}z' c_k(z, z') f(z')$. While C_0 is an ordinary in-plane conductivity, C_s describes the generation of an in-plane spin current from an electric field in the presence of surface scattering. As we show below, C_s is the essential ingredient of our theory, producing an AH current of first order in the spin Hall angle. On the other hand, C_r' and C_r'' – respectively the real and the imaginary part of the spin-mixing conductance [14] – contribute only to second order. In particular, C_r'' is the essential ingredient of the spin Hall mechanism of the AH effect [10].

In the presence of the spin-orbit scattering, the driving electric fields $\mathbf{E}, \boldsymbol{\mathcal{E}}_{\parallel}, \boldsymbol{\mathcal{E}}_{\perp}$ are self-consistently determined by the internal current densities as follows

$$\begin{aligned} \mathbf{E} &= \mathbf{E}_{ext} + \rho_{sh}\hat{\mathbf{z}}\times(\mathbf{Q}_{\parallel} - \mathbf{Q}_{\perp}) \\ \boldsymbol{\mathcal{E}}_{\parallel} &= \rho_{sh}\hat{\mathbf{z}}\times\mathbf{j} \\ \boldsymbol{\mathcal{E}}_{\perp} &= -\rho_{sh}\hat{\mathbf{z}}\times\mathbf{j} \end{aligned} \tag{2}$$

where $\rho_{sh} \equiv \rho_0\theta_{sh}$ with ρ_0 being the Drude resistivity and θ_{sh} the spin Hall angle of the metal layer. Solving

the system of linear equations (1) and (2), we obtain a general expression for the AH current density up to $O\left(\theta_{sh}^2\right)$

$$j_y\left(z\right)=\left[\rho_{sh}\left\{C_0,C_s\right\}-\rho_{sh}^2C_0C_r''C_0\right]E_{ext} \tag{3}$$

where $\{,\}$ represents the anticommutator of the two integral operators. Note that with finite C_s the AH effect appears already at the first order of θ_{sh}. The two orderings of C_0 and C_s in the anticommutator of Eq. (3) correspond to the processes b1 and b2 of Fig. 1. The second term on the right hand side of Eq. (3) corresponds to the spin Hall AH effect which is of second order in θ_{sh} and is proportional to the imaginary part of the spin-mixing conductivity kernel. In what follows, we employ the Boltzmann transport theory to explicitly construct the integral kernels C_0 and C_s in the presence of a rough magnetic interface.

Boltzmann theory−To quantitatively describe the nonlocal AH effect in a heavy metal thin layer with an external electric field applied in the $x-$direction (see Fig. 1(b)), we make use of the spinor Boltzmann equation in the relaxation time approximation [3, 15–17]

$$v_z\frac{\partial\hat{f}\left(\boldsymbol{k},z\right)}{\partial z}-eE_{ext}v_x\left(\frac{\partial\hat{f}_0}{\partial\varepsilon_k}\right)+\frac{\boldsymbol{\sigma}\cdot\left[\boldsymbol{e}_k\times\hat{\boldsymbol{\imath}}\left(k,z\right)\right]}{\tau_{so}}=-\frac{\hat{f}\left(\boldsymbol{k},z\right)-\hat{\bar{f}}\left(k,z\right)}{\tau}+\frac{2\hat{\bar{f}}\left(k,z\right)-\hat{I}Tr_\sigma\hat{\bar{f}}\left(k,z\right)}{\tau_{sf}} \tag{4}$$

where $\hat{f}_0$ and $\hat{f}\left(\boldsymbol{k},z\right)$ are 2×2 matrices represent respectively the equilibrium and nonequilibrium spinor distribution functions, $\boldsymbol{v}=\mathrm{d}\varepsilon_k/\hbar\mathrm{d}\boldsymbol{k}$ is conduction electron velocity, $\hat{\bar{f}}\left(k,z\right)\equiv\left(1/4\pi\right)\int\mathrm{d}\Omega_{\boldsymbol{k}}\hat{f}\left(\boldsymbol{k},z\right)$ is the angular average of the distribution and $\hat{\boldsymbol{\imath}}\left(k,z\right)\equiv\left(1/4\pi\right)\int\mathrm{d}\Omega_{\boldsymbol{k}}\mathbf{e}_k\hat{f}\left(\boldsymbol{k},z\right)$ is its dipolar moment, with $\boldsymbol{e}_k$ the unit vector of $\boldsymbol{k}$. Non-spin-flip and spin-slip processes are included, with τ and τ_{sf} being the momentum and spin relaxation times respectively. The additional source term $\tau_{so}^{-1}\boldsymbol{\sigma}\cdot\left[\boldsymbol{e}_k\times\hat{\boldsymbol{\imath}}\left(k,z\right)\right]$, where τ_{so}^{-1} is the spin-orbit scattering rate, is responsible for the spin Hall effect [18–20]. It is this term that generates the current-dependent fields in Eq. (2).

The crucial step in our theory is the description of spin-dependent interfacial scattering via boundary conditions for the distribution function. For the interface (at $z=0$) between the heavy metal and the ferromagnetic insulator, we impose the following generalized Fuchs-Sondheimer boundary condition [21],

$$\hat{f}^+(\boldsymbol{k},0)=\frac{1}{2}\hat{s}\hat{R}^\dagger\hat{f}^-(\boldsymbol{k},0)\hat{R}+\frac{1}{2}\left(\hat{I}-\hat{s}\right)\left\langle\hat{f}^-(\boldsymbol{k},0)\right\rangle+h.c. \tag{5}$$

where $h.c.$ represents hermitian conjugate which ensures $\hat{f}^+$ to be an hermitian, $\hat{I}$ is the 2×2 identity matrix, $\left\langle\hat{f}\right\rangle=\left(2\pi\right)^{-1}\int\mathrm{d}\phi_{\boldsymbol{k}}\hat{f}$ with $\phi_{\boldsymbol{k}}$ the $\boldsymbol{k}$-space azimuthal angle, and both $\hat{s}$ and $\hat{R}$ are 2×2 matrices in spin space which are responsible for spin dependent specular reflection and spin rotation of incident electrons.

The matrix $\hat{R}$, satisfying $\hat{R}^\dagger\hat{R}=\hat{I}$, is the reflection amplitude matrix which captures the spin rotation of electrons that are *specularly reflected* from the magnetic interface (Note that we assume such a coherent spin rotation does not occur for the diffusively scattered electrons). The explicit form of $\hat{R}$ can be determined by electron wave function matching subject to the following *spin-dependent* potential barrier

$$\hat{V}\left(z\right)=\left(V_b\hat{I}-J_{ex}\hat{\sigma}_z\right)\Theta\left(-z\right) \tag{6}$$

where V_b is the averaged potential barrier of the insulator, J_{ex} measures the spin splitting of the energy barrier, $\hat{\sigma}_z$ is the $z-$component of the Pauli spin matrices, and $\Theta\left(z\right)$ is the unit step function. Explicitly, $\hat{R}$ takes the following form (see Appendix B for the derivation)

$$\hat{R}=\left(\frac{R^\uparrow+R^\downarrow}{2}\right)\hat{I}+\left(\frac{R^\uparrow-R^\downarrow}{2}\right)\hat{\sigma}_z \tag{7}$$

where $R^\sigma=-\left(\kappa^\sigma+ik_z\right)/\left(\kappa^\sigma-ik_z\right)$ with k_z the $z-$component of the electron wave vector, $\kappa^\sigma\equiv\sqrt{2m_e^*\left(V_b-\sigma J_{ex}\right)-k_z^2}$ (we have let $\hbar=1$ for notation convenience) and m_e^* being the electron effective mass.

The matrix $\hat{s}$, on the other hand, is introduced to describe the averaged effects of spin dependent scattering at the magnetic interface due to roughness, impurities, etc. In general, we write [22, 23]

$$\hat{s}=s_0\left(\hat{I}+p_s\hat{\sigma}_z\right) \tag{8}$$

where $s_0\equiv\left(s^\uparrow+s^\downarrow\right)/2$ is the average of the specular reflection coefficients $s^\uparrow$ and $s^\downarrow$ for spin-up and spin-down electrons with "up" and "down" defined with respect to $\mathbf{m}\left(=\hat{\mathbf{z}}\right)$, and $p_s\equiv\left(s^\uparrow-s^\downarrow\right)/\left(s^\uparrow+s^\downarrow\right)$ is their asymmetry. A simple model calculation for the rough interface yields (see Appendix B for the detailed calculation), to the lowest order in J_{ex}/V_b, the specular reflection asymmetry $p_s\simeq-\frac{2J_{ex}}{V_b}\left(1-s_0\right)$ for $s_0\lesssim1$. Note that p_s

is *negative*, meaning that more spin-down electrons are specularly scattered than spin-up electrons, for the former encounter a higher energy barrier. Also, we notice that a rough magnetic interface is essential for the spin asymmetry of the specular reflection coefficients: for an ideally flat interface, both $s^{\uparrow}$ and $s^{\downarrow}$ are exactly equal to one, and no charge/spin conversion can occur.

For the outer surface at $z = d$, we assume, for simplicity, that the scattering is diffusive, i.e.,

$$\hat{f}^{-}(\boldsymbol{k},d) = \left\langle \hat{f}^{+}(\boldsymbol{k},d) \right\rangle \tag{9}$$

Note that the boundary conditions given by Eqs. (5) and (9) demand that both charge and spin currents flowing along the z-direction vanish at the outer (non magnetic) surface, whereas only the charge current and the z-component of the spin current flowing along the z-direction vanish at the magnetic surface.

By solving the Boltzmann equation (4) with the boundary conditions given by Eqs. (5) and (9), we have calculated the current densities in the heavy-metal layer. Up to first order in $\theta_{sh}(\equiv \tau/\tau_{so})$, the Hall current density can be expressed as follows

$$j_y^{ah}(z) = \rho_{sh} E_{ext} \int_0^d \frac{\mathrm{d}z'}{l_e} \left[c_s(z,z')\, \bar{c}_0(z') + c_0(z,z')\, \bar{c}_s(z') \right] \tag{10}$$

where l_e is the electron mean free path, the nonlocal integral kernels $c_s(z,z')$ and $c_0(z,z')$ are given by

$$c_0(z,z') = \frac{3}{4} \int_0^1 \mathrm{d}\xi \left(\xi^{-1} - \xi\right) \left(s_0 e^{-\frac{z+z'}{l_e \xi}} + e^{-\frac{|z-z'|}{l_e \xi}} \right) \tag{11}$$

and

$$c_s(z,z') = \frac{3}{4} p_s \int_0^1 \mathrm{d}\xi \left(\xi^{-1} - \xi\right) s_0 e^{-\frac{z+z'}{l_e \xi}} \tag{12}$$

with their spatial averages defined as $\bar{c}_0(z) \equiv \int_0^d \frac{\mathrm{d}z'}{l_e} c_0(z,z')$ and $\bar{c}_s(z) \equiv \int_0^d \frac{\mathrm{d}z'}{l_e} c_s(z,z')$. The nonlocality of the AH effect, i.e., the spatial separation of the spin-orbit scattering and the magnetization, is clearly reflected in the structure of these integral kernels which depend on the relative distance between the current and field points as well as the distance of their center of mass coordinate from the interface. Equations (10)-(12) are the main results of this paper.

One of the most remarkable features of the nonlocal AH effect is that it appears at the first order of the spin Hall angle, which is distinctly different from the spin Hall AH effect which occurs at the second order. Since p_s is negative, the directions of the nonlocal AH and the spin Hall AH currents would be the *same* for positive θ_{sh} but the *opposite* for negative θ_{sh}, as can be seen from Eq. (3). Furthermore, the nonlocal AH is independent of spin diffusion and thus is present in both ballistic and diffusive regimes, whereas the spin Hall AH effect vanishes as the thickness of the metal layer becomes much smaller than the spin diffusion length [10].

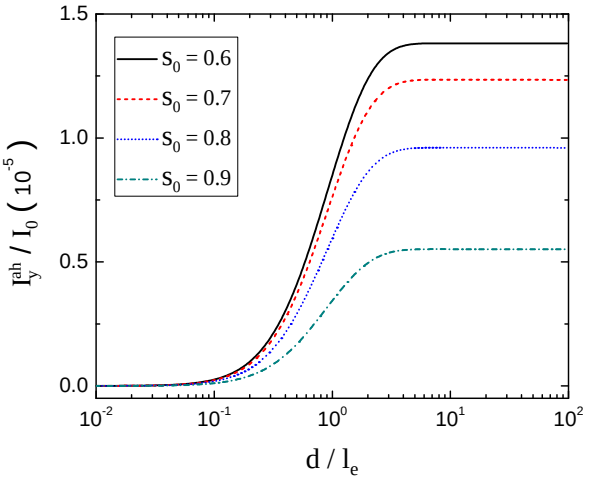

FIG. 2: The ratio of total AH current I_y^{ah} to I_0 $(= c_0 E_{ext} w d)$ as a function of the thickness of the heavy metal layer for several specular reflection parameters. Other Parameters: $\theta_{sh} = 0.05$, $J_{ex} = 0.01\ eV$ and $V_b = 12\ eV$.

The total AH current can be calculated from Eq. (10) by integrating the AH current density over the thickness of the layer, i.e., $I_y^{ah}(d) \equiv w \int_0^d \mathrm{d}z j_y^{ah}(z)$ with w being the width of the metal bar. By doing so, we find $I_y^{ah}(d) = 2\rho_{sh} E_{ext} w \int_0^d \frac{\mathrm{d}z'}{l_e} \bar{c}_s(z')\, \bar{c}_0(z')$ where the factor of 2 shows that the two physical processes that we described in Fig. 1b contribute *equally* to the total AH current. In Fig. 2, we show the thickness dependence of the total AH current for several values of the specular reflection coefficient. We find that I_y^{ah} begins to saturate when the thickness reaches the electron mean free path. Also, we note that the saturation current is smaller for a smoother surface (larger s_0), as expected from the above discussions.

Experimentally, a most relevant quantity is the ratio of the spatially averaged AH resistivity to the longitudinal resistivity, i.e., $\theta_{ah} \equiv \bar{\rho}_{xy}^{ah}(d) / \bar{\rho}_{xx}(d)$. The AH resistivity can be obtained by inverting the conductivity tensor. Since $p_s s_0 \theta_{sh} \lesssim 10^{-1}$, to a good approximation, we can take $\bar{\rho}_{xy}^{ah} \simeq \bar{c}_{xy}^{ah} / \bar{c}_{xx}^{2}$ where $\bar{c}_{xy}^{ah} \equiv d^{-1} \int_0^d \mathrm{d}z j_y^{ah}(z) / E_{ext}$ with $j_y^{ah}(z)$ given by Eq. (10). In Fig. 3, we show the thickness dependence of θ_{ah} for several values of the specular reflection coefficient s_0. For $d \ll l_e$, θ_{ah} tends to zero, because $\bar{\rho}_{xx}(d)$ increases with decreasing layer thickness. In the opposite limit of $d \gg l_e$, θ_{ah} also diminishes since the nonlocal AH effect is essentially an interface effect, which saturates for thicknesses larger than the electron mean path. By choosing the following parameters for a Pt $(7\ nm)$/YIG bilayer at room temperature:

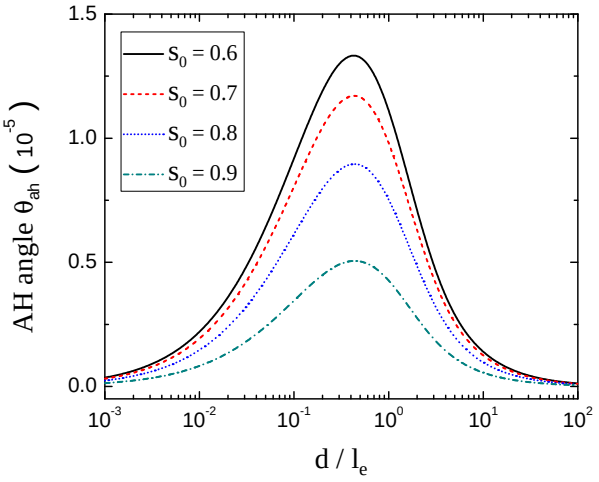

FIG. 3: The AH angle θ_{ah} ($\equiv \bar{\rho}^{ah}_{xy}(d)/\bar{\rho}_{xx}(d)$) as a function of thickness of the heavy metal layer for several values of the specular reflection coefficient. Other Parameters: $\theta_{sh} = 0.05$, $J_{ex} = 0.01\ eV$ and $V_b = 12\ eV$.

$\theta_{sh} = 0.05$ [24], $s_0 = 0.6$, $J_{ex} = 0.01\ eV$ [25], $V_b = 12\ eV$and $l_e = 20\ nm$[13], we estimate the AH angle arising from our mechanism to be about 1.3×10^{-5}, which is in good agreement with experimental observations [6, 7].

As a final point, we suggest a crucial verification of our mechanism by contrasting the directions of the Hall current (or the signs of Hall voltages) of two trilayer structures Pt/Cu/YIG and β-Ta/Cu/YIG. Since the spin Hall angles of Pt and β-Ta are of opposite signs [26–28] we predict that the Hall current directions in these two trilayers will be opposite. A Cu layer, thinner than the electron mean free path, may be inserted between the heavy-metal and the magnetic insulator in order to eliminate the magnetic proximity effect, while the nonlocal AH effect will still be operative.

Acknowledgement.—It is a pleasure to thank O. Heinonen, S. Zhang, A. Hoffmann, W. Jiang and W. Zhang for various stimulating discussions. One of the author, S. S.-L. Zhang is deeply indebted to O. Heinonen for his hospitality at Argonne National Lab, where part of the work was done. This work was supported by NSF Grants DMR-1406568.

Appendix A: Spinor reflection amplitude at a metal/magnetic-insulator interface

Consider the following free electron Hamiltonian for a metal/magnetic-insulator interface

$$\hat{H} = \frac{\hat{\mathbf{p}}^2}{2m_e^*} + \left(V_b \hat{I} - J_{ex}\hat{\sigma}_z\right)\Theta(-z) \tag{A1}$$

where V_b is the spin-averaged barrier for electrons to go from the metal to the insulator, J_{ex} is the exchange coupling which is responsible for the spin-splitting of energy levels in the insulator, and $\Theta(z)$ is the unit step function. Here we have chosen the spin quantization axis to be parallel to the magnetization $\mathbf{m}$ ($= \hat{\mathbf{z}}$). For an incident electron (from the metal side, $z > 0$) with its spin pointing in the direction (θ, ϕ) with respect to $\mathbf{m}$, we can write the scattering wave function as follows

$$\hat{\psi}(\mathbf{r}) = \cos\left(\frac{\theta}{2}\right) e^{-i\phi/2}\varphi^{\uparrow}(\mathbf{r})\,|\uparrow\rangle + \sin\left(\frac{\theta}{2}\right) e^{i\phi/2}\varphi^{\downarrow}(\mathbf{r})\,|\downarrow\rangle \tag{A2}$$

where the spatial parts of the spinor wave function are

$$\varphi^{\sigma}(\mathbf{r}) = \begin{cases} \left(e^{-ik_z z} + R^{\sigma}e^{ik_z z}\right)e^{i\mathbf{q}\cdot\boldsymbol{\rho}}, & z > 0 \\ T^{\sigma}e^{\kappa^{\sigma} z}e^{i\mathbf{q}\cdot\boldsymbol{\rho}}, & z < 0 \end{cases} \tag{A3}$$

where $\sigma = \uparrow$ ($\downarrow$), R^{σ} and T^{σ} are the corresponding reflection and transmission amplitudes, $\mathbf{k} = (\mathbf{q}, k_z)$ and $\mathbf{r} = (\boldsymbol{\rho}, z)$ are the wave vector and spatial coordinates respectively, and $\kappa^{\sigma} = \sqrt{k_b^2 - \sigma k_J^2 - k_z^2}$ with $k_b \equiv \sqrt{2m_e^* V_b/\hbar^2}$ and $k_J \equiv \sqrt{2m_e^* J_{ex}/\hbar^2}$. By matching the wave functions and their derivatives at $z = 0$, we find

$$R^{\sigma} = -\frac{\kappa^{\sigma} + ik_z}{\kappa^{\sigma} - ik_z} \tag{A4}$$

and

$$T^{\sigma} = 1 + R^{\sigma} = -\frac{2ik_z}{\kappa^{\sigma} - ik_z}. \tag{A5}$$

Appendix B: Spin dependent specular reflection coefficient

In this section, we prove that the specular reflection coefficient s is spin-dependent for a rough metal/magnetic-insulator interface. In the absence of interface roughness, the bilayer can be modeled as a simple spin-dependent step potential as given in Eq. (A1), the corresponding free electron Green's function (setting $\hbar = 1$) reads

$$g^{\sigma}_{\mathbf{q}}(z, z'; E) = \frac{m_e^*}{ik_z}\left[e^{ik_z|z-z'|} + R^{\sigma}e^{-ik_z(z+z')}\right] \tag{B1}$$

where $z < 0$ and $z' < 0$, $k_z = \sqrt{2m_e^* E - q^2}$ with E the total kinetic energy and $\mathbf{q}$ the in-plane momentum, and the reflection amplitude for electron with spin σ is given by Eq. (A4).

Now we model a rough interface by a set of randomly-distributed impurities localized at the interface ($z = 0$) with δ-correlated potential $V_{imp}(\mathbf{r})$ satisfying the following properties [29–31]

$$\langle V_{imp}(\mathbf{r})\rangle = 0 \tag{B2}$$

and

$$\langle V_{imp}(\mathbf{r})\, V_{imp}(\mathbf{r}')\rangle = \gamma\delta(\boldsymbol{\rho} - \boldsymbol{\rho}')\,\delta(z)\,\delta(z') \tag{B3}$$

where $\langle\rangle$ denotes the impurity ensemble average and γ describes the amplitude of the fluctuation. Up to first order in γ, the *impurity-averaged* Green's function reads [30]

$$\left\langle G^{\sigma}_{\mathbf{q}}(z,z';E)\right\rangle = g^{\sigma}_{\mathbf{q}}(z,z';E) + \gamma g^{\sigma}_{\mathbf{q}}(z,0;E) g^{\sigma}_{\mathbf{q}}(0,z';E) N^{\sigma}(0;E) \quad \text{(B4)}$$

where $N^{\sigma}(0;E) \equiv \int \frac{\mathrm{d}\mathbf{q}'}{(2\pi)^2} g^{\sigma}_{\mathbf{q}'}(0,0;E)$. By placing Eq. (B1) into Eq. (B4), we find

$$\left\langle G^{\sigma}_{\mathbf{q}}(z,z';E)\right\rangle = \frac{m}{ik_z}\left\{ e^{ik_z|z-z'|} + e^{-ik_z(z+z')} R^{\sigma}\left[1 - 2i\gamma N^{\sigma}(0;E)\frac{k_z}{U^{\sigma}_b}\right]\right\} \quad \text{(B5)}$$

where $U^{\sigma}_b \equiv V_b - \sigma J_{ex}$ is the spin-dependent barrier. Comparing Eq. (B5) with Eq. (B1), we identify the effective reflection amplitude in the presence of the surface roughness as

$$\bar{R}^{\sigma} = R^{\sigma}\left[1 - 2i\gamma N^{\sigma}(0;E)\frac{k_z}{U^{\sigma}_b}\right] \quad \text{(B6)}$$

Up to $O(\gamma)$, the reflection coefficient is

$$r^{\sigma} = |R^{\sigma}|^2\left[1 - 2\gamma A^{\sigma}(0;E)\frac{k_z}{U^{\sigma}_b}\right] \quad \text{(B7)}$$

with the surface spectral function defined as $A^{\sigma}(0;E) = -2\Im m\, N^{\sigma}(0;E)$. We thus identify the specular reflection coefficient as

$$s^{\sigma} = 1 - 2\gamma A^{\sigma}(0;E)\frac{k_z}{U^{\sigma}_b} \quad \text{(B8)}$$

By placing Eq. (B1) into Eq. (B8) and carrying out the integration over in-plane momentum $\mathbf{q}$, we obtain an explicit expression for s^{σ}

$$s^{\sigma} = 1 - \gamma\frac{2k_z\left(2m^*_e E\right)^{3/2}}{3\pi\left(U^{\sigma}_b\right)^2} \simeq 1 - \gamma\frac{2k_z k_F^3}{3\pi V_b^2}\left(1 + \sigma\frac{2J_{ex}}{V_b}\right) \quad \text{(B9)}$$

where we have replaced the total kinetic energy E by the Fermi energy and kept term up to $O(J_{ex}/V_b)$. Therefore, we have shown that the specular reflection coefficient is indeed spin-dependent. We also note that s_{σ} is in general dependent on the *direction* of the incident momentum. For brevity, we shall work with an angle-averaged specular reflection coefficient, i.e.,

$$\bar{s}_{\sigma} = \int \mathrm{d}\Omega_{\mathbf{k}} s_{\sigma}(q)/4\pi = 1 - \frac{\gamma k_F^4}{3\pi^2 V_b^2}\left(1 + \sigma\frac{2J_{ex}}{V_b}\right) \quad \text{(B10)}$$

It follows that the spin averaged specular reflection coefficient as well as the spin symmetry of the specular reflection can be expressed as (up to $O(J_{ex}/V_b, \gamma)$)

$$s_0 \equiv \frac{\bar{s}^{\uparrow} + \bar{s}^{\downarrow}}{2} = 1 - \gamma\cdot\frac{k_F^4}{3\pi^2 V_b^2} \quad \text{(B11)}$$

and

$$p_s \equiv \frac{\bar{s}^{\uparrow} - \bar{s}^{\downarrow}}{\bar{s}^{\uparrow} + \bar{s}^{\downarrow}} \simeq -\gamma\cdot\frac{J_{ex}}{V_b}\cdot\frac{2k_F^4}{3\pi^2 V_b^2} \quad \text{(B12)}$$

Interestingly, we note the p_s has a negative sign; in other words, the specular reflection coefficient for spin-up electrons is smaller than that of the spin-down electrons as the latter encounter a higher barrier.

Eliminating the parameter γ from Eqs. (B11) and (B12), we find an approximate relation between s_0 and p_s

$$p_s \simeq -\frac{2J_{ex}}{V_b}(1 - s_0) \quad \text{(B13)}$$

This relation is valid for a moderately rough interface, i.e., $s_0 \lesssim 1$.

[1] N. Nagaosa, J. Sinova, S. Onoda, A. H. MacDonald, and N. P. Ong, *Rev. Mod. Phys.*, **82**, 1539 (2010).
[2] J. E. Hirsch, *Phys. Rev. Lett.*, **83**, 1834 (1999).
[3] S. Zhang, *Phys. Rev. Lett.*, **85**, 393 (2000).
[4] G. Vignale, *J. Supercond. Novel Magn.*, **23**, 3 (2010).
[5] J. Sinova, S. O. Valenzuela, J. Wunderlich, C. H. Back, and T. Jungwirth, *ArXiv e-prints* (2014).
[6] S. Y. Huang, X. Fan, D. Qu, Y. P. Chen, W. G. Wang, J. Wu, T. Y. Chen, J. Q. Xiao, and C. L. Chien, *Phys. Rev. Lett.*, **109**, 107204 (2012).
[7] M. Althammer, S. Meyer, H. Nakayama, M. Schreier, S. Altmannshofer, M. Weiler, H. Huebl, S. Geprägs, M. Opel, R. Gross, D. Meier, C. Klewe, T. Kuschel, J.-M. Schmalhorst, G. Reiss, L. Shen, A. Gupta, Y.-T. Chen, G. E. W. Bauer, E. Saitoh, and S. T. B. Goennenwein, *Phys. Rev. B*, **87**, 224401 (2013).
[8] B. F. Miao, S. Y. Huang, D. Qu, and C. L. Chien, *Phys. Rev. Lett.*, **112**, 236601 (2014).
[9] H. Nakayama, M. Althammer, Y.-T. Chen, K. Uchida, Y. Kajiwara, D. Kikuchi, T. Ohtani, S. Geprägs, M. Opel, S. Takahashi, R. Gross, G. E. W. Bauer, S. T. B. Goennenwein, and E. Saitoh, *Phys. Rev. Lett.*, **110**, 206601 (2013).
[10] Y.-T. Chen, S. Takahashi, H. Nakayama, M. Althammer, S. T. B. Goennenwein, E. Saitoh, and G. E. W. Bauer, *Phys. Rev. B*, **87**, 144411 (2013).
[11] E. Saitoh, M. Ueda, H. Miyajima, and G. Tatara, *Appl. Phys. Lett.*, **88**, 182509 (2006).
[12] T. Kimura, Y. Otani, T. Sato, S. Takahashi, and S. Maekawa, *Phys. Rev. Lett.*, **98**, 156601 (2007).
[13] G. Fischer, H. Hoffmann, and J. Vancea, *Phys. Rev. B*, **22**, 6065 (1980).
[14] A. Brataas, Y. V. Nazarov, and G. E. W. Bauer, *Phys. Rev. Lett.*, **84**, 2481 (2000).

[15] T. Valet and A. Fert, *Phys. Rev. B*, **48**, 7099 (1993).
[16] J. Zhang, P. M. Levy, S. Zhang, and V. Antropov, *Phys. Rev. Lett.*, **93**, 256602 (2004).
[17] Y. Qi and S. Zhang, *Phys. Rev. B*, **67**, 052407 (2003).
[18] E. M. Hankiewicz and G. Vignale, *Phys. Rev. B*, **73**, 115339 (2006).
[19] S. K. Lyo and T. Holstein, *Phys. Rev. Lett.*, **29**, 423 (1972).
[20] E. G. Mishchenko and B. I. Halperin, *Phys. Rev. B*, **68**, 045317 (2003).
[21] S. S.-L. Zhang, G. Vignale, and S. Zhang, *Phys. Rev. B*, **92**, 024412 (2015).
[22] R. E. Camley and J. Barnaś, *Phys. Rev. Lett.*, **63**, 664 (1989).
[23] R. Q. Hood, L. M. Falicov, and D. R. Penn, *Phys. Rev. B*, **49**, 368 (1994).
[24] L. Liu, R. A. Buhrman, and D. C. Ralph, *ArXiv e-prints* (2011).
[25] Y. Kajiwara, K. Harii, S. Takahashi, J. Ohe, K. Uchida, M. Mizuguchi, H. Umezawa, H. Kawai, K. Ando, K. Takanashi, S. Maekawa, and E. Saitoh, *Nature*, **464**, 262 (2010).
[26] L. Liu, C.-F. Pai, Y. Li, H. W. Tseng, D. C. Ralph, and R. A. Buhrman, *Science*, **336**, 555 (2012).
[27] M. Morota, Y. Niimi, K. Ohnishi, D. H. Wei, T. Tanaka, H. Kontani, T. Kimura, and Y. Otani, *Phys. Rev. B*, **83**, 174405 (2011).
[28] C. Hahn, G. de Loubens, O. Klein, M. Viret, V. V. Naletov, and J. Ben Youssef, *Phys. Rev. B*, **87**, 174417 (2013).
[29] X.-G. Zhang and W. H. Butler, *Phys. Rev. B*, **51**, 10085 (1995).
[30] D. A. Stewart, W. H. Butler, X.-G. Zhang, and V. F. Los, *Phys. Rev. B*, **68**, 014433 (2003).
[31] V. F. Los, *Phys. Rev. B*, **72**, 115441 (2005).